

RESEARCH

Open Access



Predicting pathological response of locally advanced breast cancer to neoadjuvant chemotherapy: comparing the performance of whole body ^{18}F -FDG PETCT versus DCE-MRI of the breast

Alaa Sobhi^{*} , Soha Talaat hamed, El-shaymaa Hussein, Shaimaa Lasheen, Mai Hussein and Youstina Ebrahim

Abstract

Background: With the expansion of the use of the neoadjuvant chemotherapy (NAC) in locally advanced breast cancer (LABC), both dynamic contrast enhanced magnetic resonance imaging (DCE-MRI) and ^{18}F -fluorodeoxyglucose positron emission tomography (^{18}F -FDG PET CT) are promising methods for assessment of the tumor response during chemotherapy. We aimed to evaluate the diagnostic accuracy of DCE-MRI of breast & ^{18}F -FDG PETCT regarding the assessment of early response to neoadjuvant chemotherapy (NAC) in locally advanced breast cancer patients (LABC) and pathological complete response (pCR) prediction.

Results: A total of forty LABC patients who had NAC were included in the study. Before and during NAC, PET/CT and DCE-MRI were used. Various morphological and functional criteria were compared and linked with post-operative pathology for both. The MRI sensitivity and specificity in assessing NAC response in conjunction with pathological data were 100% ($p=0.001$) and 12.5% ($p=0.18$) respectively. The equivalent readings for PET/CT were 94.1% ($p=0.001$) and 25% ($p=0.18$), respectively, although the estimated total accuracy for both MRI and PETCT was the same measuring 94.1% ($p=0.001$) and 25% ($p=0.18$) (72%). PETCT had a higher overall accuracy than MRI in assessing the response of axillary lymph nodes (ALN) to NAC (64% and 56%, respectively). Longest diameter of lesion, ADC value, and maximal enhancement in baseline MRI, SUV_{max} and SUV_{mean} in baseline PETCT were all significant predictors of rCR.

Conclusion: During NAC in the primary breast mass and ALN, DCE-MRI demonstrated a better sensitivity in predicting pCR in LABC patients. Although both MRI and PETCT were equally accurate in detecting pCR of LABC patients to NAC, PETCT was more accurate in detecting pathological response of ALN to NAC.

Keywords: PETCT, MRI breast, Locally advanced breast cancer, Neoadjuvant chemotherapy, Assessment of response, Post-operative pathology

Background

Over the last few decades, the use of neoadjuvant chemotherapy (NAC) to improve surgical results has increased. It has also been demonstrated that establishing a pathological complete response (pCR) after NAC is associated

*Correspondence: Alaa.Radio2013@gmail.com
Women's Imaging Unit, Radiology Department, Nuclear Medicine and Clinical Oncology Departments, Kasr Al Ainy Hospital, Cairo University, Manial, Cairo, Egypt

with a better disease-free survival rate, particularly in her2 enriched and triple negative breast cancer [1].

With the widespread use of NAC in breast cancer treatment, it's more important than before to assess response early and precisely in order to guide future management and forecast pCR [2].

Dynamic contrast-enhanced MRI is a morphological and functional imaging, morphological through (tumour size and cellularity, i.e. shrinkage pattern) and functional changes (through diffusion-weighted images, perfusion MRI, and spectroscopy) [3].

FDG PET/CT is used to assess primary tumour extent and detect metastases in breast cancer patients. It can also provide functional information about tumour metabolism, allowing for earlier identification of response to therapy than the more delayed gross morphological changes seen on conventional imaging [4].

The goal of this study was to compare the diagnostic accuracy of DCE-MRI of the breast and 18 F-FDG PETCT in assessing NAC response in locally advanced breast cancer patients, as well as to analyze their effectiveness as pCR predictors.

Methods

The Radiology, Nuclear Medicine, and Clinical Oncology Departments were collaborated on this prospective study from January 2019 to February 2020. The work was authorized by the institutional review board's Ethical committee. Patients had given their informed consent.

Patients who were going to get NAC were screened. Patients were included in the study if they met the following criteria: female gender, age (18–70 years), and pathologically established primary LABC were also factors to consider (stage II–III). The following criteria were used to exclude people: Patients with recognized contraindications to 18F-FDG-PET/CT&/or DCE-MRI, such as pregnancy and renal insufficiency, should not undergo the procedure, patients who were not candidates for NAC and those who were diagnosed with metastatic breast cancer.

Recent guidelines from the U.S. National Comprehensive Cancer Network describe LABC as AJCC stage III breast cancer; the definition includes breast cancer that fulfils any of the following criteria in the absence of distant metastasis [5]:

- Tumors more than 5 cm in size with regional lymphadenopathy (N1–3)
- Tumors of any size with direct extension to the chest wall or skin, or both (including ulcer or satellite nodules), regardless of regional lymphadenopathy
- Presence of regional lymphadenopathy (clinically fixed or matted axillary lymph nodes, or any of infra-

clavicular, supraclavicular, or internal mammary lymphadenopathy) regardless of tumor stage.

Radiological versus pathological response

In our study, our reference of tumoral response was the post-operative pathology. According to the post-operative pathology, tumoral response was classified into complete response (pCR) and incomplete response (non-pCR).

We monitored the response during treatment by two radiological modalities, MRI and PET/CT scan. Therefore, in each modality we assessed the radiological response and classified patients according to the radiological findings into radiological complete response (rCR) and radiological incomplete response (non-rCR). In terms of Breast MRI, the response has been evaluated using RECIST 1.1 criteria. While in PET/CT, the response has been assessed using the PERCIST 1.0 criteria.

We finally correlated the radiological response to the pathological response to evaluate the accuracy of each radiological modality in assessment of tumoral response.

Included patients were subjected to both baseline and interim DCE -MRI of breast and whole body PETCT to evaluate the response and determine the rCR of the tumor and the axillary nodal disease. The diagnostic performance of both modalities were compared and then correlated with post-operative pathology.

Treatment was comprised of anthracyclin-taxane based chemotherapy for 8 cycles. Trastuzumab was added to taxanes in Her2 positive cases.

DCE-MRI

A 1.5-T scanner (Achieva, Philips) with a specialised bilateral breast coil was used for the MRI. Patients were scanned while lying down. Axial sequences in a row Thrive in three dimensions T1-weighted sequences ($1.1 \times 1.1 \times 1.1$ mm³ voxels; 90 s acquisition time; TR/TE 4.4/2.3 ms, flip angle 10 mm, FOV 360 mm) were obtained. Initial enhancement (90s after contrast agent injection), late enhancement (450 s after contrast agent injection), maximum intensity projections, and dynamic curves assessment were all done with subtraction images. Diffusion Weighted Images (DWIs) were included in our research, as well as an ADC map.

In DCE-MRI, the longest diameter of: (a) Enhancing lesions in DCE-MRI was measured to assess NAC response using RECIST 1.1 criteria. (b) Bright Lesions in DWIs "Restricted Diffusion". This equation was used to calculate the relative change in tumour size on MRI (RECIST 1.1) (Table 1).

Table 1 Criteria for evaluation of response of breast lesions and axillary lymph nodes by DCE-MRI versus PET/CT

Response category	Response Evaluation Criteria in Solid Tumors (RECIST 1.1) (Eisenhauer et al. 2009) [23]	PET Response Criteria in Solid Tumors (PERCIST) (Wahl et al. 2009) [24]
Complete response (CR)	Disappearance of all target lesions Reduction in short axis of target lymph nodes to < 10 mm	Disappearance of all lesions on PET images to background blood-pool levels, regardless of % change from baseline and anatomic size
Partial response (PR)	≥ 30% decrease in sum of target lesion diameter sum	≥ 30% decrease in sum of target lesion SUV
Progressive disease (PD)	≥ 20% increase in sum of target lesion diameter and minimum of 5 mm total increase or new lesion or unequivocal progression of non-target lesions	30% increase in sum of target lesion SUV or new FDG avid lesion or unequivocal progression of non-target lesion (e.g., ≥ 30% increase) or unequivocal progression by RECIST
Stable disease (SD)	Does not meet other criteria	Does not meet other criteria
Axillary lymph nodes assessment	Malignant lymph nodes: To be considered pathologically enlarged and measurable, a lymph node must be ≥ 15 mm in short axis. At baseline and in follow-up, only the short axis will be measured and followed	Follow the same criteria as the breast lesions regarding SUV change (CR, PR, PD and SD)

$$\frac{\text{Largest diameter interim MRI} - \text{Largest diameter baseline}}{\text{MRI Largest diameter baseline MRI}} \times 100\%$$

The lesion location and a full descriptive study of its enhancement were documented both for MRI pre NAC and post NAC, according to the literature Hobb et al. [6] and the Breast Imaging-Reporting and Data System (BI-RADS) lexicon.

According to El Kassas et al. [7], lesions' ADC values were evaluated, along with all b values (0, 850, 1000). We integrated ADC map views with DCE-MRI at this time to characterize the lesions and measure ADC values in the relevant hypo-intense areas on the ADC map. Each ROI's mean ADC was calculated.

18F-FDG-PET/CT

The European Association of Nuclear Medicine (EANM) procedural guidelines for FDG PET/CT tumour imaging: version 2.07 were used to conduct whole-body 18F-FDG-PET/CT studies [8]. Before imaging, patients were told to fast for at least 4 hours and receive intravenous 18F-FDG

injections of 4.62MBq/kg (0.125mCi/kg) up to 555MBq (15mCi). Blood glucose levels should be fewer than 200 mg/dL on the day of the research. The scanner employed in this investigation is the Philips Healthcare Ingenuity TF 64, which combines a modular, LYSO-based design. A qualitative (visual) and quantitative evaluation were carried out. With a thresholding method of 40% of SUV max in the ROI, we estimated several metrics of the primary breast mass.

The metabolic response was assessed by comparing relative changes in the SUVmax, SUV Mean, MTV (Metabolic tumour volume), and TLG (Total lesion glycolysis).

After two cycles of NAC, patients were assessed for response using PET Response Criteria in Solid Tumors (PERCIST) 1.0, which was based on 18F-FDG PET/CT data (Table 1). An equation similar to that employed by Hatt et al. [4] was used to compute the relative change in maximum standardized uptake value (SUVmax).

(See figure on next page.)

Fig. 1 Clinical data: A 33-year-old woman with right breast cancer(T2N1). Histologic findings demonstrated grade II invasive ductal carcinoma (Triple negative). Post-operative pathologic findings revealed dense fibrosis and adenosis with no viable tumor tissue (complete pathological response) that confirmed with lumpectomy(yptON0). **A** The first row figure: (a–c) Breast MR images prior to neoadjuvant chemotherapy demonstrate a 1.6 × 1.2 cm oval circumscribed enhancing mass in the right breast on axial post-contrast (a) images restricted diffusion (b) with an ADC value of 0.5 (c). The second row (d–f) Breast MR images during neoadjuvant chemotherapy demonstrate complete regression in size of the previously noted right breast mass (d), with no evidence of areas of diffusion restriction in DWI and ADC images (e, f). Complete response. "Complete response". **B** The first row 18FDG-PET/CT images prior to chemotherapy demonstrate a metabolically active 18FDG avid hyper-dense well defined rounded mass in the right breast on (a)axial CT, (b) axial PET and (c) axial fused PET/CT images (SUVmax=8.3, SUVmean=4.7, MTV=2.4, TLG=11). The second row (d–f) 18FDG-PET/CT images during chemotherapy demonstrate complete metabolic and anatomic response of the previously detected known right breast mass on (d) axial CT, (e) axial PET and (f) axial fused PET/CT images."Complete response"

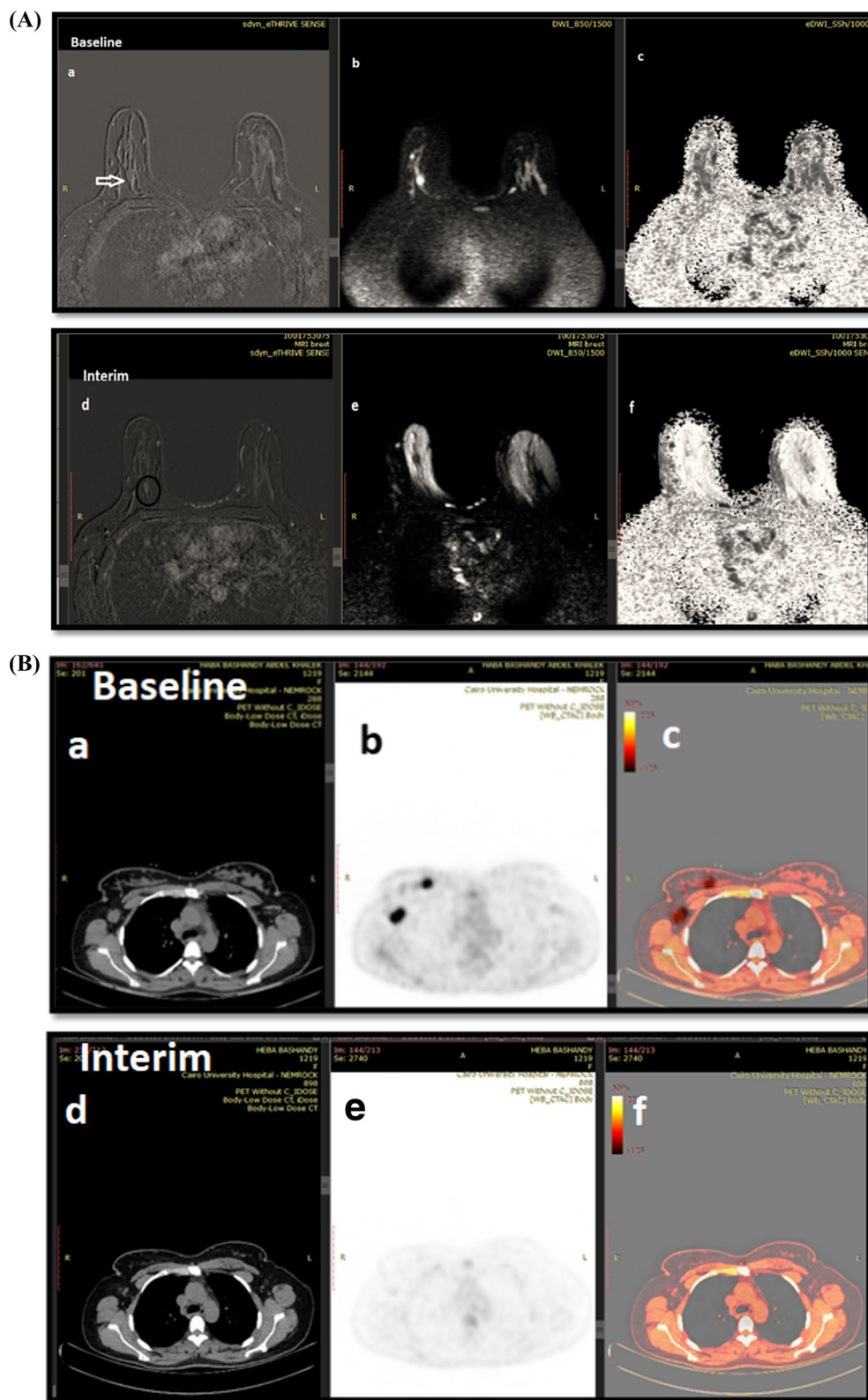


Fig. 1 (See legend on previous page.)

$$\% \text{ SUVmax} = \frac{[(\text{SUVpre} - \text{SUVpost})]}{\text{SUVpre}} \times 100\%$$

Patients with NAC underwent surgical treatment, either MRM or BCS. The patients were classified either pathological complete response (pCR), that defined as either complete absence of tumor cells or presence of only a small number of scattered invasive cells in the breast resection specimen (Fig. 1) or Pathological non-complete response (non-pCR) that defined as any remaining viable residual disease in the breast due to partial tumor response, stable or progressive disease [9] (Fig. 2).

Statistical methods

The Statistical Package for Social Sciences (SPSS) ver. 25 was used to handle and analyse the data. For independent groups, the Student t-test was used to compare numerical variables that were normally distributed and the Mann-Whitney U test was used to compare numerical variables that were not normally distributed. The Chi square test or Fisher's exact test were used to compare categorical data as needed. Both MRI and PET/CT diagnostic accuracy (sensitivity and specificity) as well as positive and negative predictive values were assessed. A receiver operator characteristic (ROC) analysis was used to establish the diagnostic discrimination for predicting pathologic response by various imaging modalities.

Results

Although forty patients were screened initially, fifteen patients were excluded from the study (Eight were missing interim MRI or PET/CT due to the current COVID pandemic, six patients had bone metastasis on baseline PET/CT and one patient withdrew the consent).

The final analysis included twenty-five cases. The patients' average age at the time of diagnosis was 45.8 years. Only eight of the patients attained pCR, whereas the other seventeen did not achieve pCR in correlation with post-operative pathology.

IDC was found in 24 cases, while ILC was found in only one. Clinical stage IIb was present in 32% of the patients, although clinical stage III was present in 68%. Only over 25% of hormone receptor positive/HER 2 negative (luminal) cases achieved pCR, whereas 44.4% of HER2+ve/triple negative patients achieved pCR.

Twelve of the 25 patients had a modified radical mastectomy, while the other thirteen had breast conservation surgery.

The maximum diameter of the lesion, maximum enhancement percentage, and ADC value were the only parameters that linked with pCR in the baseline MRI before NACT, with *p* values of 0.027, 0.001, and 0.043, respectively. The lesion was described in interim MRI in the same way as it did in the first MRI, however the only statistically significant parameter was the time to peak of contrast uptake (in seconds), which had a median value of 235.0 sec. The change in tumour size and maximal enhancement regression were the only statistically significant parameters when compared to baseline MRI, with *p* values of 0.016 and 0.049, respectively. (Table 2).

In MRI, a cut-off initial longest diameter of 4.25 was proposed for discriminating rCR from non-rCR patients. AUC was 77.9. Cut-off values of initial SUVmax, SUV mean, ADC, maximum enhancement were not applicable, although there was a statistical significance as the area under the curve was very small and unreliable (Fig. 5).

The maximum and mean standardized uptake values (SUVmax & SUVmean), MTV, and TLG were assessed at baseline PET/CT. The SUVmax and SUVmean parameters were statistically significant (*p* values of 0.027 and 0.016, respectively). In relation to pCR, however, none of the PET/CT values at interim PET/CT, nor the computed difference between the two scans, approached statistical significance (Table 3).

(See figure on next page.)

Fig. 2 Clinical data: A 48-year-old woman with left breast cancer (T3N1). Histologic findings demonstrated grade II invasive ductal carcinoma (luminal B1). Post-operative pathology revealed IDC grade I with low grade DCIS with partial effect to therapy confirmed with BCS(ypt1N1). **A** The first row (a–c) Breast MR images prior to neoadjuvant chemotherapy demonstrate a 3 × 2.8 cm irregular microlobulated enhancing mass in the left breast on axial post-contrast (a) images restricted diffusion (b) with an ADC value of 0.9 (c). The second (d–f) Breast MR images during neoadjuvant chemotherapy demonstrate partial regression in size of the previously noted left breast mass with inserted clips seen within, measuring 2.4 × 2.2 cm (d), with still restricted diffusion signal in DWI with ADC value about 1.2 in images (e) (f). Δ diameter of lesion = 20% regression. “Stable disease”. **B** The first row is 18FDG-PET/CT images prior to neoadjuvant chemotherapy demonstrate a metabolically active 18FDG avid hyper-dense irregular speculated mass in the left breast on (a) axial CT, (b) axial PET and (c) axial fused PET/CT images (SUVmax = 9.9, SUVmean = 5.7, MTV = 28.8, TLG = 164.1). The second row (d–f) 18FDG-PET/CT images during chemotherapy metabolic progression of such lesion, however anatomic regression noted on (d) axial CT, (e) axial PET and (f) axial fused PET/CT images (SUVmax = 11.5, SUVmean = 6.7, MTV = 5.2, TLG = 34.8, ΔSUVmax = 13.9% progression) “progressive disease”

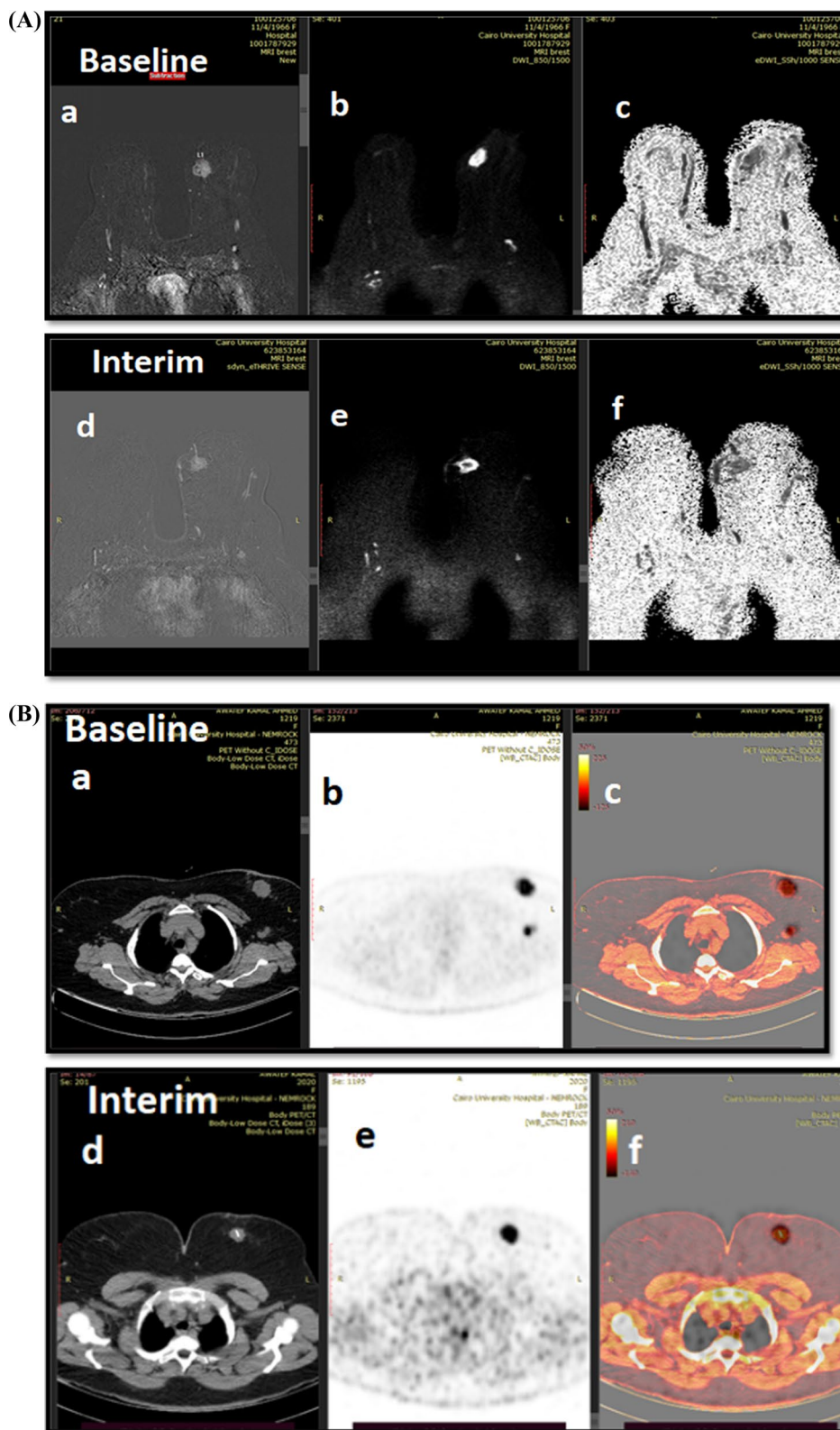


Fig. 2 (See legend on previous page.)

Table 2 Results of MRI parameters in relation to pathologic response (n = 25)

	pCR (n = 8)		Non-pCR (n = 17)		p value
	Median	(Range)	Median	(Range)	
MRI baseline					
Max. diameter (cm)	3.8	(1.6–5.6)	5.5	(2.5–15.0)	0.027
ADC value	0.5	(0.3–0.9)	0.4	(0.3–0.8)	0.711
Max. enhancement %	123.5	(66.0–185.0)	72.0	(8.0–102.0)	0.001
MRI interim					
Max. diameter (cm)	2.8	(1.9–5.0)	3.5	(1.3–12.0)	0.576
ADC value	0.8	(0.4–1.2)	0.5	(0.3–3.0)	0.711
Max. enhancement %	52.5	(25.0–117.0)	40.0	(8.5–90.0)	0.288
MRI (baseline vs interim)					
Max. diameter (cm) regression %	30.5	(8.0–100.0)	35.0	(4.0–64.0)	0.016
ADC % change	37.5	(25.0–79.0)	16.7	(0.0–84.0)	0.932
Max. enhancement regression %	56.0	(12.0–79.0)	21.0	(0.0–84.0)	0.049

Bold means the parameter was significant p-value < 0.05

Table 3 Results of PET/CT parameters in relation to pathologic response (n = 25)

	pCR (n = 8)		Non-pCR (n = 17)		p value
	Median	(Range)	Median	(range)	
PET/CT Initial					
SUV max	8.8	(5.4–16.0)	5.7	(2.1–12.9)	0.027
SUV mean	4.9	(2.7–5.7)	2.7	(1.1–6.2)	0.016
MTV	19.3	(2.4–32.0)	20.8	(5.1–128.1)	0.406
TLG	96.9	(8.7–166.4)	61.4	(9.7–584.5)	0.798
PET/CT Interim					
SUV max	2.9	(1.4–16.0)	2.5	(1.0–7.4)	0.581
SUV mean	1.9	(1.0–10.2)	1.8	(0.7–4.0)	0.731
MTV	5.2	(1.2–15.5)	7.4	(1.1–32.4)	0.407
TLG	6.1	(1.2–86.7)	17.6	(2.8–198.9)	0.490
PET/CT (baseline vs interim)					
SUV _{max} regression %	70.5	(0.0–100.0)	52.0	(25.0–100.0)	0.754
SUV _{mean} regression %	60.0	(96.2–100.0)	39.3	(0.0–84.0)	0.157
MTV % change	79.0	(47.0–100.0)	73.0	(5.0–100.0)	0.440
TLG regression %	86.0	(47.0–100.0)	82.0	(23.0–100.0)	0.588

Bold means the parameter was significant p-value < 0.05

(See figure on next page.)

Fig. 3 Clinical data: A 46-year-old woman with right breast cancer (T3N1). Histologic findings demonstrated grade II invasive ductal carcinoma (luminal B1). Post-operative pathologic findings revealed IDC grade I with low grade DCIS with partial effect to therapy confirmed with BCS(ypt1N1). **A** The first row is (a–c) Breast MR images prior to neoadjuvant chemotherapy demonstrate a 4.6 × 3.9 cm irregular microlobulated enhancing mass in the left breast on axial post-contrast (a) images restricted diffusion (b) with an ADC value of 0.9 (c). The second row (d–f) Breast MR images during neoadjuvant chemotherapy demonstrate partial regression in size of the previously noted left breast mass, measuring 2.9 × 2.5 cm (d), with still restricted diffusion signal in DWI with ADC value about 1 in images (e, f). Δ diameter of lesion = 37% regression “partial response”. **B** The first row is 18FDG-PET/CT images prior to neoadjuvant chemotherapy demonstrate a metabolically active 18FDG avid hyper-dense irregular microlobulated mass in the left breast on (a) axial CT, (b) axial PET and (c) axial fused PET/CT images (SUV_{max} = 5.2, SUV_{mean} = 5.2, MTV = 32, TLG = 166). The second row (d–f) 18FDG-PET/CT images during chemotherapy demonstrate metabolic stability, however anatomic regression in the previously detected known left breast mass on (d) axial CT, (e) axial PET and (f) axial fused PET/CT images (SUV_{max} = 2.47, SUV_{mean} = 10.26, MTV = 8.5, TLG = 86.7. ΔSUV_{max} = 54% regression) “partial response”

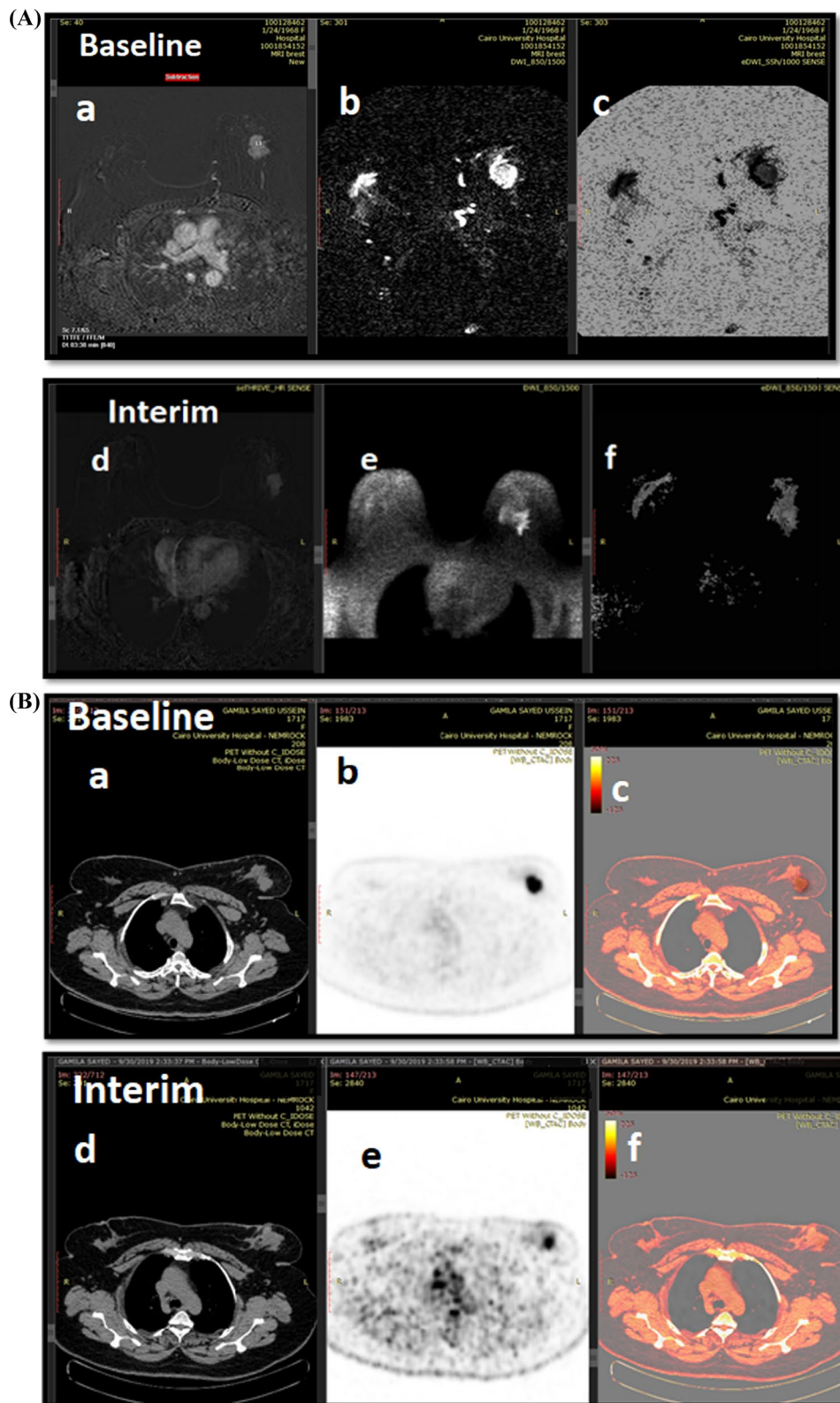


Fig. 3 (See legend on previous page.)

Comparison of tumor responses; radiologic versus pathologic response

PET CT assessment after two cycles of NACT, using relative reduction in SUVmax parameter (according to PERCIST), revealed 3 patients to be rCR i.e. not traced in images “complete radiological response” and 22 non-rCR. Among 3 rCR (in correlation with post operative pathology) we found that two of them were true negative (TN) (Fig. 1), however only one was false negative (FN). Among 22 non-rCR, 16 were true positive (TP) (Figs. 2, 3) and 6 were false positive (FP) (Fig. 4) (p value=0.016).

On the other hand, DCE-MRI assessment after two cycles of NACT, using relative reduction in longest diameter parameter (according to RECIST), revealed one patient to be rCR and 24 were non-rCR. The one rCR is true negative (TN) (Fig. 1), among 24 non-rCR, 7 were false positive (FP) (Fig. 4) and 17 were true positive (TP) (Figs. 2, 3) (p value=0.125).

The response to neo-adjuvant therapy in axillary lymph nodes were assessed by RECIST and PERCIST criteria in MRI and PETCT respectively (Table 1).

The sensitivity and specificity of MRI in assessing ALN response to NAC in association with pathological data were (83% and 50%) respectively, however the corresponding values in PET/CT were (47.4% and 68.4%) respectively. PETCT, on the other hand, was predicted to have a higher overall accuracy than MRI (64% and 56%) respectively (Table 4). MRI was significant in detection axillary lymph nodes in relation to pathological response ($p=0.012$) (Table 5).

Discussion

During Neoadjuvant chemotherapy NAC, accurate assessment of the presence or absence of residual tumors can guide the range of surgical resection, avoiding radical mastectomy and increasing the possibility of breast-conserving surgery. Furthermore, correct assessment may aid the clinician in adjusting the chemotherapy regimen for patients who have a suboptimal response [10].

In this study, regarding the baseline MRI, we found that the longest diameter of the lesion, ADC value and percentage of maximum enhancement were statistically significant in prediction of pathological response ($p=0.027$, 0.043 and 0.001 respectively).

Mansour et al [11] also found that the ADC value as a single parameter to predict pCR achieved 78.95% sensitivity, 83.33% specificity and 80.65% total accuracy. The additive role of DWI to conventional DCE-MRI enhanced the diagnostic indices to 89.47% sensitivity, 83.87% total accuracy (compared to 73.68% and 77.42%, respectively, in case of DCE-MRI alone).

While in interim MRI the peak of contrast uptake and change in tumor size (pre-post/post $\times 100$) as well as change in maximum enhancement were significant radiological prognostic factors for prediction of pCR ($p < 0.05$), However change in ADC value was not statically significant ($p=0.932$).

Bouzón et al [12] found that MRI can accurately measure tumor response and residual tumor size in breast cancer patients treated with NAC. In their series, evaluation of residual tumor size was more accurate in baseline tumor size ≤ 5 cm lesions, similar to our results. Scheel et al [13] also found that change in size in MRI between pre-NAC and during NAC can be used to guide the implementation of chemotherapy regimens. Minarikova et al. [14] found that the change in tumor size as measured by MRI served as a significant predictor of CR compared to change in ADC values which was similar to our conclusion (Fig. 5).

In this study, the positive predictive value of MRI breast (ability to correctly predict the presence of residual disease at final pathologic examination) was found to be 70.8%, however the negative predictive value (ability to correctly predict the absence of disease at final pathologic examination) was found to be only 58.8%. In a meta-analysis of six investigations, Crashaw et al. [15] discovered that MRI has a high positive predictive value (93%). Because the negative predictive value was only moderate (65%), the overall diagnostic accuracy was reduced to (84%).

(See figure on next page.)

Fig. 4 Clinical data: A 38-year-old woman with left breast cancer (T3N0). Histologic findings demonstrated grade III invasive ductal carcinoma (triple negative). Post-operative pathologic findings revealed complete absence of tumor cells, wide areas of necrosis as well as free surgical margins confirmed with BCS(ypt0N0). **A** the first row is (a–c) Breast MR images prior to neoadjuvant chemotherapy demonstrate a 5 \times 3.9 cm irregular macro-lobulated rim enhancing mass in the left breast on axial post-contrast (a) images restricted diffusion (b) with an ADC value of 0.4 (c). The second row (d–f) Breast MR images during neoadjuvant chemotherapy demonstrate significant regression in size of the previously noted left breast mass, leaving behind linear non mass enhancement, measuring 1.4 \times 1.2 cm (d), with still restricted diffusion signal in DWI with ADC value about 0.4 in images (e, f). Δ diameter of lesion = 58% regression “partial response”. **B** The first row is 18FDG-PET/CT images prior to chemotherapy demonstrate a metabolically active 18FDG avid hyper-dense well circumscribed rounded mass in the left breast on (a) axial CT, (b) axial PET and (c) axial fused PET/CT images (SUVmax = 12.9, SUVmean = 3.8, MTV = 72.6, TLG = 376). The second row (d–f) 18FDG-PET/CT images during chemotherapy demonstrate significant metabolic and anatomic regression in the previously detected left breast mass with clips seen within the mass on (d) axial CT, (e) axial PET and (f) axial fused PET/CT images (SUVmax = 4, SUVmean = 1.6, MTV = 32.4, TLG = 52.4, Δ SUVmax = 68.9% regression) “partial response”

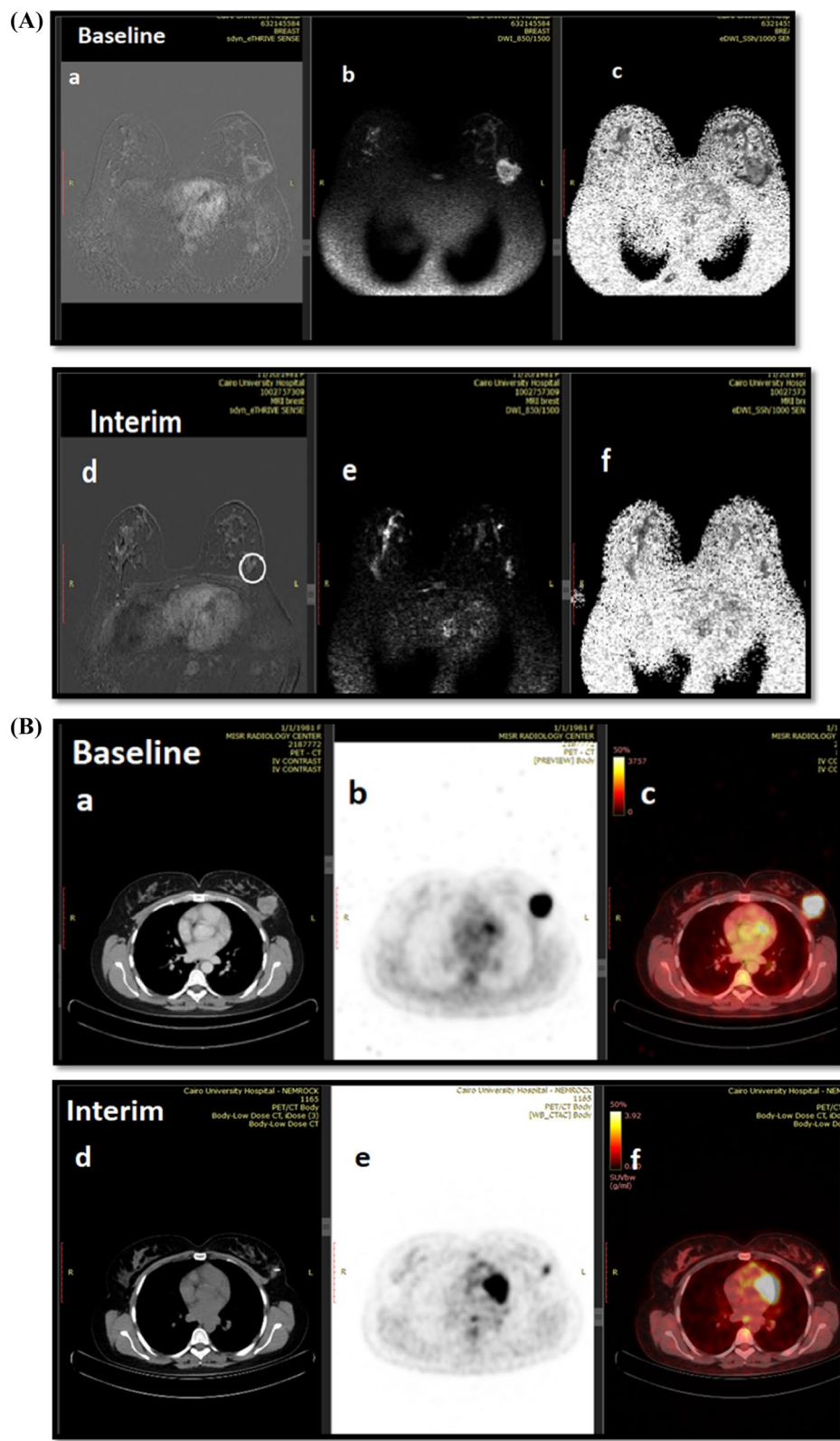


Fig. 4 (See legend on previous page.)

Table 4 Diagnostic performance of MRI versus PET/CT

Parameter	MRI (%)	PET/CT (%)	p value ^a
Sensitivity	100.0	94.1	<0.001
Specificity	12.5	25.0	0.180
Positive predictive value	70.8	72.7	NA
Negative predictive value	100.0	66.7	NA

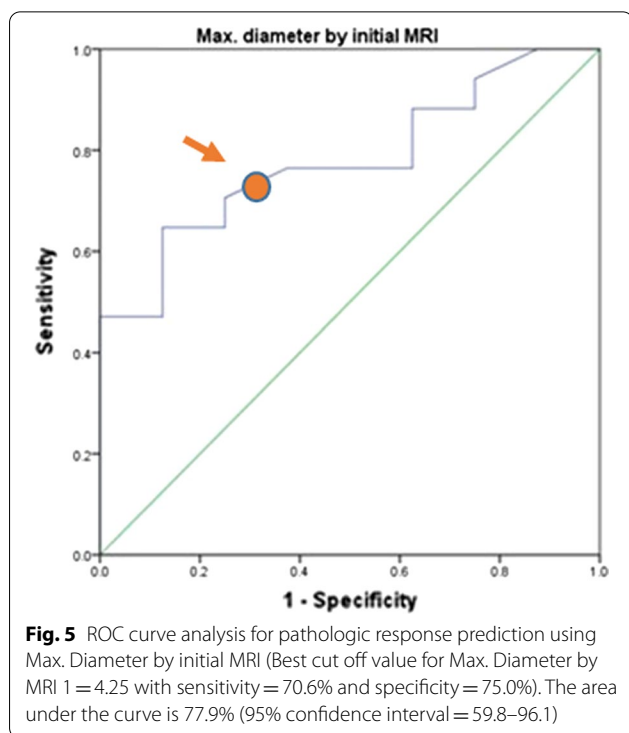
^a Chi-square/ Fisher exact test

Table 5 Comparison of axillary LN status detected by radiologic versus pathologic modalities (n = 25)

Radiology	Pathology		p value ^a
	Positive (n = 6)	Negative (n = 19)	
MRI			
Positive	5	10	0.012
Negative	1	9	
PET/CT			
Positive	3	6	0.508
Negative	3	13	

Bold means the parameter was significant p-value < 0.05

^a Chi-square/ Fisher exact test



In terms of PET/CT, the original 18F-FDG-PET/CT upstaged five cases to stage IV disease (advanced disease); it identified previously undiscovered distant

metastatic disease in bones, particularly in the axial skeleton, impacting treatment options considerably. This was consistent with level II evidence that supports the use of 18F-FDG PET/CT for initial staging of patients with LABC since it enhanced both regional and systemic staging [16]. SUV_{max} and SUV_{mean} of the breast mass in the initial pre-therapy scan were the only statistically significant metabolic factors in predicting rCR, with P values of 0.027 and 0.016 respectively, according to semi-quantitative analysis of 18F-FDG-PET CT. However, no other deduced quantitative metabolic parameters were statistically significant in the interim PET scan nor the calculated difference between both scans (a calculated according to the PERCIST).

We calculated MTV and TLG of the primary breast mass with thresholding method of 40% of SUV max in the ROI and they were not significant either in the initial or the interim scans, this could be explained by Hong et al. [17] who stated that MTV and TLG may be two promising metabolic parameters. However, selecting a verified appropriate threshold to delineate the tumour and calculate volume-based factors appears to be difficult, given the various clinical contexts such as lesions size, tumour biology, and background breast activity that can be modified by patient age and hormonal status.

In comparison to pathological data, the pooled sensitivity and specificity of MRI in assessing LABC response to neoadjuvant therapy were 100% (p0.001) and 12.5% (p=0.18), respectively. The corresponding figures for PET/CT were 94.1% (p0.001) and 25% (p=0.18), respectively. However, the total accuracy for both MRI and PET/CT was 72%. Breast MR imaging was found to be a sensitive medium for breast cancer identification and an accurate imaging method for assessing tumour response to neoadjuvant therapy by Mariscotti et al. [18]. In patients with breast cancer, Li et al. [19] discovered that MRI had a higher sensitivity and PET/CT had a higher specificity for predicting the pathologic response following NAC, similar to our findings.

Sarhan et al. [20] had evaluated the role of FDG-PET/CT in assessment of response to NAC in breast cancer, they found that the sensitivity, specificity, and accuracy of PET.CT were 95.5%, 75%, and 90%, respective values, the higher specificity and hence the accuracy of the study could be attributed to two essential differences. Firstly, they analyzed PET based-parameters after end of NAC not in the early interim phase as our study: this may raise the awareness of the added value of PET/CT after end of therapy regarding the specificity of the study, to avoid higher incidence of false positive results in interim PET due to associated early therapy related inflammatory changes.

Secondly, Sarhan et al. [20] used SUV values corrected to lean body mass (SUL) which can overcome many

shortcomings related to SUV corrected to body weight as it is not affected with changes in patient's body weight which may be encountered due to effect of therapy [21].

The sensitivity and specificity of MRI in assessing the response of axillary lymph nodes to neoadjuvant therapy in association with pathological data were 83% and 50%, respectively, in the current investigation. The corresponding values for PET/CT were 47.4% and 68.4%, respectively, with p values of ($p = 0.625$) and ($p = 0.146$), but the estimated overall accuracy of PET/CT was higher than that of MRI (64% and 56%, respectively), which was similar to Ergul et al. [22] who reported that PET/CT had a higher specificity for detecting axillary nodal involvement than MRI (89%).

The limitations in our study was the limited number of patients that resulting in defect in assessment the different imaging modalities for assessment response to NAC as well as performing subgroup analysis based on receptor subtypes.

Conclusion

We concluded that DCE-MRI and 18 F-FDG-PET CT could play different roles in the evaluation of NAC in LABC patients as;

- DCE-MRI had a higher sensitivity in predicting the pCR in locally advanced breast cancer after NAC either in the primary breast mass or the axillary lymph nodes (ALN), although there was no difference in overall accuracy in the former, however PET/CT was more accurate in the latter.
- 18 F-FDG-PET/CT had therapeutic implication by measuring baseline metabolic activity in the primary tumor and ALN and by detecting distant metastatic disease not previously disclosed by conventional imaging modalities.

Abbreviations

ALN: Axillary lymph nodes; ADC: Apparent diffusion coefficient; BIRADS: Breast Imaging-Reporting and Data System; CR: Complete response; DCE-MRI: Dynamic contrast enhanced Magnetic resonance imaging; DWI: Diffusion weighted images; EANM: European Association of Nuclear Medicine; FDG: Fluoro-deoxy-glucose; LABC: Locally advanced breast cancer; MTV: Metabolic tumor volume; NAC: Neoadjuvant chemotherapy; Non-pCR: Pathological incomplete response; Non-rCR: Radiological incomplete response; NPV: Negative predictive value; pCR: Pathological complete response; PD: Progressive disease; PERCIST: PET response criteria in solid tumors; PET/CT: Positron emission tomography/computed tomography; PPV: Positive predictive value; PR: Partial response; rCR: Radiological complete response; RECIST: Response evaluation criteria in solid tumors; ROI: Region of interest; SD: Stable disease; SUV: Standardized uptake value; SUV_{Max} : Maximum SUV; TLG: Total lesion glycolysis.

Acknowledgements

We would like to acknowledge the head of Women's imaging unit, Radiology department, Cairo University; Prof. Dr. Rasha Kamal who always support the research works. And we would like to acknowledge Dr. Manal Ali Basha, resident of general surgery, Cairo University, for great help and her kind and co-operation.

Authors' contributions

SA is the guarantor of integrity of the entire study. TS, HE and SA contributed to the study concepts and design. TS, SA, HE and EY contributed to the literature research. SA, TS, HE and HM contributed to the clinical studies. All authors contributed to the experimental studies/data analysis. SA and LS contributed to the statistical analysis. SA and LS contributed to the manuscript preparation. SA, TS and LS contributed to the manuscript editing. All authors read and approved the final manuscript.

Funding

No funding was obtained for this study.

Availability of data and materials

The corresponding author is responsible for sending the used data and materials upon request.

Declarations

Ethics approval and consent to participate

The study was approved by the ethical committee of the Radiology Department of Kasr –Al-Ainy Hospital, Cairo University which is an academic governmental supported highly specialized multidisciplinary Hospital. The included patients gave written informed consent.

Committee's reference number

Not applicable.

Consent for publication

All patients included in this research were legible, above 16 years of age. They gave written informed consent to publish the data contained within this study.

Competing interests

The authors declare that they have no competing interests.

Received: 30 August 2021 Accepted: 4 March 2022

Published online: 31 March 2022

References

1. Cortazar P, Zhang L, Untch M, Mehta K, Costantino JP, Wolmark N, Bonnefoi H, Cameron D, Gianni L, Valagussa P, Swain SM, Prowell T, Loibl S, Wickerham DL, Bogaerts J, Baselga J, Perou C, Blumenthal G, Blohmer J, Von Minckwitz G (2014) Pathological complete response and long-term clinical benefit in breast cancer: the CTNeoBC pooled analysis. *Lancet* 384(9938):164–172. [https://doi.org/10.1016/S0140-6736\(13\)62422-8](https://doi.org/10.1016/S0140-6736(13)62422-8)
2. Rauch GM, Adrada BE, Kuerer HM, Van La Parra RFD, Leung JWT, Yang WT (2017) Multimodality imaging for evaluating response to neoadjuvant chemotherapy in breast cancer. *Am J Roentgenol* 208(2):290–299. <https://doi.org/10.2214/AJR.16.17223>
3. Al-Hilli Z, Boughey JC (2016) The timing of breast and axillary surgery after neoadjuvant chemotherapy for breast cancer. *Chin Clin Oncol* 5(3):1–11. <https://doi.org/10.21037/cco.2016.03.26>
4. Hatt M, Groheux D, Martineau A, Espié M, Hindíé E, Giacchetti S, De Roquancourt A, Visvikis D, Cheze-Le Rest C (2013) Comparison between 18F-FDG PET image-derived indices for early prediction of response to neoadjuvant chemotherapy in breast cancer. *J Nucl Med* 54(3):341–349. <https://doi.org/10.2967/jnumed.112.108837>
5. National Comprehensive Cancer Network (NCCN) (2015) NCCN clinical practice guidelines in oncology: breast cancer. NCCN, Fort Washington

6. Hobbs MM, Taylor DB, Buzynski S, Peake RE (2015) Contrast-enhanced spectral mammography (CESM) and contrast enhanced MRI (CEMRI): patient preferences and tolerance. *J Med Imaging Radiat Oncol* 59(3):300–305. <https://doi.org/10.1111/1754-9485.12296>
7. El Kassas H, Helal M, Abourabia A, Abd El Razik N, Farahat A, Zedan M (2016) Role of MRI diffusion as an adjunct to contrast enhanced MRI of the breast for the evaluation of breast cancer patients receiving neoadjuvant chemotherapy. *Egypt J Radiol Nucl Med* 47(4):1721–1732. <https://doi.org/10.1016/j.ejrnm.2016.06.003>
8. Boellaard R, Delgado-Bolton R, Oyen WJG, Giammarile F, Tatsch K, Eschner W, Verzijlbergen FJ, Barrington SF, Pike LC, Weber WA, Stroobants S, Delbeke D, Donohoe KJ, Holbrook S, Graham MM, Testanera G, Hoekstra OS, Zijlstra J, Visser E, Krause BJ (2015) FDG PET/CT: EANM procedure guidelines for tumour imaging: version 2.0. *Eur J Nucl Med Mol Imaging* 42(2):328–354. <https://doi.org/10.1007/s00259-014-2961-x>
9. Chen JH, Feig BA, Hsiang DJ, Butler JA, Mehta RS, Bahri S, Nalcioglu O, Su MY (2009) Impact of MRI-evaluated neoadjuvant chemotherapy response on change of surgical recommendation in breast cancer. *Ann Surg* 249(3):448–454. <https://doi.org/10.1097/SLA.0b013e31819a6e01>
10. Wang H, Mao X (2020) Evaluation of the efficacy of neoadjuvant chemotherapy for breast cancer. *Drug Des Dev Ther* 14:2423–2433. <https://doi.org/10.2147/DDDT.S253961>
11. Mansour S, Selim A, Kassam L et al (2021) Diffusion-weighted imaging or MR spectroscopy: Which to use for the assessment of the response to chemotherapy in breast cancer patients? *Egypt J Radiol Nucl Med* 52:190. <https://doi.org/10.1186/s43055-021-00574-2>
12. Bouzón A, Acea B, Soler R, Iglesias Á, Santiago P, Mosquera J, Calvo L, Seoane-Pillado T, García A (2016) Diagnostic accuracy of MRI to evaluate tumour response and residual tumour size after neoadjuvant chemotherapy in breast cancer patients. *Radiol Oncol* 50(1):73–79. <https://doi.org/10.1515/raon-2016-0007>
13. Scheel JR, Kim E, Partridge SC, Lehman CD, Rosen MA, Bernreuter WK, Pisano ED, Marques HS, Morris EA, Weatherall PT, Polin SM, Newstead GM, Esserman LJ, Schnall MD, Hylton NM (2018) MRI, clinical examination, and mammography for preoperative assessment of residual disease and pathologic complete response after neoadjuvant chemotherapy for breast cancer: ACRIN 6657 trial. *Am J Roentgenol* 210(6):1376–1385. <https://doi.org/10.2214/AJR.17.18323>
14. Minarikova L, Bogner W, Pinker K, Valkovič L, Zaric O, Bago-Horvath Z, Bartsch R, Helbich TH, Trattng S, Gruber S (2017) Investigating the prediction value of multiparametric magnetic resonance imaging at 3 T in response to neoadjuvant chemotherapy in breast cancer. *Eur Radiol* 27(5):1901–1911. <https://doi.org/10.1007/s00330-016-4565-2>
15. Croshaw R, Shapiro-Wright H, Svensson E, Erb K, Julian T (2011) Accuracy of clinical examination, digital mammogram, ultrasound, and MRI in determining postneoadjuvant pathologic tumor response in operable breast cancer patients. *Ann Surg Oncol* 18(11):3160–3163. <https://doi.org/10.1245/s10434-011-1919-5>
16. Caresia Aroztegui AP, García Vicente AM, Alvarez Ruiz S, Delgado Bolton RC, Orcajo Rincon J, García Garzon JR, de Arcocha Torres M, Garcia-Velloso MJ (2017) 18F-FDG PET/CT in breast cancer: evidence-based recommendations in initial staging. *Tumor Biol* 39(10):1–23. <https://doi.org/10.1177/1010428317728285>
17. Hong JH, Kim HH, Han EJ, Byun JH, Jang HS, Choi EK, Kang JH, Yoo IR (2016) Total lesion glycolysis using 18F-FDG PET/CT as a prognostic factor for locally advanced esophageal cancer. *J Korean Med Sci* 31(1):39–46. <https://doi.org/10.3346/jkms.2016.31.1.39>
18. Mariscotti G, Houssami N, Durando M, Bergamasco L, Campanino PP, Ruggieri C, Regini E, Luparia A, Bussone R, Sapino A, Fonio P, Gandini G (2014) Accuracy of mammography, digital breast tomosynthesis, ultrasound and MR imaging in preoperative assessment of breast cancer. *Anticancer Res* 34(3):1219–1225
19. Li H, Yao L, Jin P, Hu L, Li X, Guo T, Yang K (2018) MRI and PET/CT for evaluation of the pathological response to neoadjuvant chemotherapy in breast cancer: a systematic review and meta-analysis. *Breast* 40:106–115. <https://doi.org/10.1016/j.breast.2018.04.018>
20. Sarhan EAS, El Gohary MI, El Moneim LA et al (2020) Role of 18 fluorine-fluorodeoxyglucose positron emission tomography/computed tomography in assessment of neoadjuvant chemotherapy response in breast cancer patients. *Egypt J Radiol Nucl Med* 51:116. <https://doi.org/10.1186/s43055-020-00233-y>
21. Sarikaya I, Albatineh AN, Sarikaya A (2020) Revisiting weight-normalized SUV and lean-body-mass-normalized SUV in PET studies. *J Nucl Med Technol* 48(2):163–167. <https://doi.org/10.2967/jnmt.119.233353>
22. Ergul N, Kadioglu H, Yildiz S, Yucel SB, Gucin Z, Erdogan EB, Aydin M, Muslimanoglu M (2015) Assessment of multifocality and axillary nodal involvement in early-stage breast cancer patients using 18F-FDG PET/CT compared to contrast-enhanced and diffusion-weighted magnetic resonance imaging and sentinel node biopsy. *Acta Radiol* 56(8):917–923. <https://doi.org/10.1177/0284185114539786>
23. Eisenhauer EA, Therasse P, Bogaerts J, Schwartz LH, Sargent D, Ford R, Dancey J, Arbuck S, Gwyther S, Mooney M, Rubinstein L, Shankar L, Dodd L, Kaplan R, Lacombe D, Verweij J (2009) New response evaluation criteria in solid tumours: revised RECIST guideline (version 1.1). *Eur J Cancer* 45(2):228–247. <https://doi.org/10.1016/j.ejca.2008.10.026>
24. Wahl RL, Jacene H, Kasamon Y, Lodge MA (2009) From RECIST to PERCIST: evolving considerations for PET response criteria in solid tumors. *J Nucl Med* 50(Suppl 1):122S–S150. <https://doi.org/10.2967/jnumed.108.057307>

Publisher's Note

Springer Nature remains neutral with regard to jurisdictional claims in published maps and institutional affiliations.

Submit your manuscript to a SpringerOpen® journal and benefit from:

- Convenient online submission
- Rigorous peer review
- Open access: articles freely available online
- High visibility within the field
- Retaining the copyright to your article

Submit your next manuscript at ► [springeropen.com](https://www.springeropen.com)